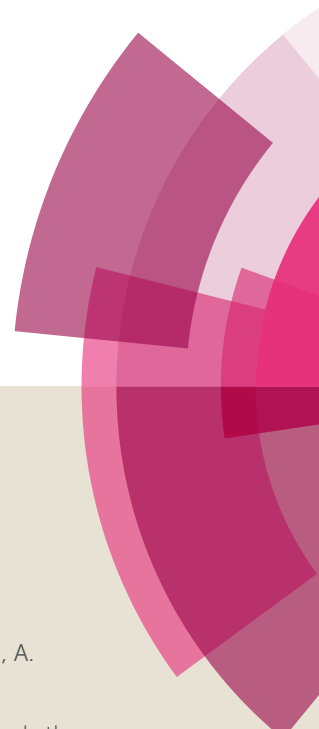


# NJC

Accepted Manuscript



This article can be cited before page numbers have been issued, to do this please use: X. Cao, Q. Ding, A. Gao, Y. Li, X. Chang and Y. Wu, *New J. Chem.*, 2018, DOI: 10.1039/C8NJ00753E.



This is an Accepted Manuscript, which has been through the Royal Society of Chemistry peer review process and has been accepted for publication.

Accepted Manuscripts are published online shortly after acceptance, before technical editing, formatting and proof reading. Using this free service, authors can make their results available to the community, in citable form, before we publish the edited article. We will replace this Accepted Manuscript with the edited and formatted Advance Article as soon as it is available.

You can find more information about Accepted Manuscripts in the [author guidelines](#).

Please note that technical editing may introduce minor changes to the text and/or graphics, which may alter content. The journal's standard [Terms & Conditions](#) and the ethical guidelines, outlined in our [author and reviewer resource centre](#), still apply. In no event shall the Royal Society of Chemistry be held responsible for any errors or omissions in this Accepted Manuscript or any consequences arising from the use of any information it contains.

# Supramolecular self-assembly material based on quinoline derivative and sensitively response toward volatile acid and organic amine vapors

Xinhua Cao<sup>\*ab</sup>, Qianqian Ding<sup>a</sup>, Aiping Gao<sup>a</sup>, Yiran Li<sup>a</sup>, Xueping Chang<sup>a</sup>, Yongquan Wu<sup>\*c</sup>

<sup>a</sup>College of Chemistry and Chemical Engineering & Henan Province Key laboratory of Utilization of Non-metallic Mineral in the South of Henan, Institute for Conservation and Utilization of Agro-bioresources in Dabie Mountains, Xinyang Normal University, Xinyang 464000, China

<sup>b</sup>State Key Laboratory of Chemo/Biosensing and Chemometrics, Hunan University, Changsha 410082, P.R. China  
E-mail: caoxhchem@163.com

<sup>c</sup>School of Chemistry and Chemical Engineering, Gannan Normal University, Ganzhou, Jiangxi 341000, P. R. China. E-mail: wyq@gnnu.edu.cn

**Abstract:** A new gelator **1** contained quinoline group was designed, synthesized and fully characterized. It was found that stable organogels **1** could be obtained in some solvents including ethanol, acetonitrile, n-hexane, petroleum ether and DMSO. It was worth mentioning that supra-gel was formed in hexane and petroleum ether with the critical gel concentration of 0.16% and 0.17%, respectively. The self-assembly process of gelator **1** in the above five solvents was carefully investigated by FESEM, UV-vis, FL, FTIR, XRD and water contact angle experiments. It was found that gelator molecule **1** could self-assembled into different self-assembly structures with different surface wettability from super-hydrophilicity to super-hydrophobicity in the self-assembly process. Organogel **1** formed in acetonitrile could emit strong light comparing with that of organogels **1** in the other four solvents under the stimulation of 365 nm light. At the same time, the fluorescence emission of organogel state had a red-shift of 70 nm comparing with that of solution state. The fluorescence emission of molecule **1** in solution and gel state was further and well verified via theoretical calculation. The fluorescence emission of gelator **1** acetonitrile solution could reversibly respond to TFA and TEA along with the change of maximum emission wavelength between 382 nm and 458 nm in turn. The xerogel **1** formed in acetonitrile exhibited sensitively responsive ability towards TFA and TEA. More interesting, the different change behavior of the fluorescence emission of molecule **1** in solution and xerogel state under responsive towards TFA and TEA. This research will provide a new way for designing multi-functional soft matter for response volatile acid and organic amine vapors.

**Keywords:** supramolecular chemistry, self-assembly, gel, volatile acid, organic amine

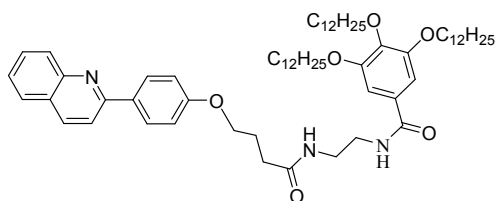
## Introduction

Supramolecular gels have obtained a great development over the past few decades due to their wide potential application in many fields such as sensor, liquid crystals, light-harvesting system, cell culture, catalysis, pollutant removal, drug delivery and materials science<sup>1-9</sup>. Supramolecular gels can be formed under the driving force of noncovalent interactions including  $\pi$ - $\pi$  stacking, hydrogen-bonding, electrostatic forces, hydrophobic interactions, van der Waals forces, coordination interactions, charge-transfer, and so on<sup>10, 11</sup>. On the base of noncovalent interactions, supramolecular gels could be prepared into multi-stimulation responsive materials via introduction of different functional groups which can be responsive to external stimuli such as metal ions, biomolecule, light, pH, enzymes, and redox agents, ultrasound, heat, electricity, mechanical action and magnetism<sup>12, 13</sup>. Many functional groups were introduced into molecular structure and constructed supramolecular gel system including carbohydrates, peptides, cholest, urea-derivatives, long alkyl chain and simple fatty acids<sup>14-17</sup>. Simultaneously, low weight organic molecule can be self-assembled into various supramolecular architectures such as core-shells, fibers, tubes, ribbons, balls, vesicles, films and honeycombs which can immobilize and then gelate a large volume of solvents in their three dimensional networks<sup>18</sup>. In this respect, we have recently reported a novel class of supramolecular gels based on naphthalimides derivatives with the sensing ability towards nitroaromatic compounds or organic amine<sup>19-21</sup>.

Volatile acids such as hydrochloric acid and trifluoroacetic acid (TFA) can be harmful to the body. For example, they can give rise to bronchial spasm, inflammation, oedema, chemical pneumonia, pulmonary edema and death if inhalation<sup>22, 22</sup>. Organic amines as important raw materials or intermediates are widely used in chemical industry, food and fine chemical engineering<sup>24</sup>. Volatile organic amines such as triethylamine (TEA) and aniline are important gaseous pollutants because they seriously damage the ecological environment and cause severe threats to human health<sup>25</sup>. Recently, several supramolecular self-assembly system exhibited the detection ability of aromatic amine or acid vapors. Xue and coworkers have reported an cyano-substituted vinylacridine derivatives linked with N-dodecyl-L-phenylalaninamide through succinyl (PC2VA) and glutaryl (PC3VA) groups which could quantitatively detect aromatic amine and volatile acid vapors caused by the low HOMO energy level of the fluorophore and the existence of the acridine moiety as an acid binding site<sup>26</sup>. We have prepared an organogel system based on an iridium complex and a Eu (III) hybrid with the ability of responsive volatile acid and organic amine vapors<sup>27</sup>.

Quinoline derivatives were widely used to be designed as fluorescence sensor or complex ligand due to their excellent coordination ability toward metal ions<sup>28, 29</sup>. Zhang and Li reported a series of 3d transition metal

complexes with a julolidine–quinoline based ligand and studied their structures, spectroscopy and optical properties<sup>30</sup>. Song and coworkers reported a quinolin oximes with ability of selective and visual detection of a nerve agent mimic by phosphorylation and protonation<sup>31</sup>. Fan and Yang reported a simple quinolone Schiff-base containing CHEF based fluorescence ‘turn-on’ chemosensor for distinguishing Zn<sup>2+</sup> and Hg<sup>2+</sup> with high sensitivity, selectivity and reversibility<sup>32</sup>. Inspired by the previous works, a new self-assembly system based on quinoline derivative was designed (Scheme 1). The molecule could be self-assembled into organogels in some solvents and exhibit AIE during gelation in acetonitrile solvent. The fluorescence emission peaks of compound **1** acetonitrile solution could have a large difference of 77 nm before and after addition of TFA. At the same time, the fluorescence emission of compound **1** acetonitrile solution could reversibly transform back the original state after addition of TEA. The fluorescence emission of the xerogel of the compound could be sensitively responded towards acids and aromatic amines through different fluorescence emission change behavior. Thus, this smart supramolecular self-assembly system may provide a new method of designing excellent multi-responsive soft matter for detection of gaseous analytes.



**Scheme 1** Molecule structure of compound **1**.

## Experimental

### Reagents and materials

2-bromoquinoline, 4-hydroxyphenylboronic acid, methyl 4-bromobutanoate, ethane-1,2-diamine and gallicin were all purchased from Shanghai Titan Scientific Co., Ltd. N,N'-Dicyclohexylcarbodiimide (DCC), 1-hydroxybenzotriazole (HOBt), trifluoroacetic acid, lithium hydroxide monohydrate and triethylamine were provided by Zhengzhou Alfa chem Co., Ltd. All other reagents were analytically pure.

### The gelation test

The compound and solvent were put in a septum-capped test tube and heated (>80 °C) until the solid was dissolved. The sample vial was then cooled to 25 °C (room temperature). Qualitatively, gelation was considered successful if no sample flow was observed upon inversion of the container at room temperature (the inverse flow method)<sup>33</sup>. Xerogels were obtained by evaporation of solvent from the gel via freeze drying.

### Instrumentation conditions

$^1\text{H}$  NMR and  $^{13}\text{C}$  NMR spectra were recorded on a Bruker-Avance (Bruker, Ltd., Switzerland), at 400 and 100 MHz, respectively. Proton chemical shifts are reported in parts per million downfield from tetramethylsilane. HRMS was recorded on a LTQ-Orbitrap mass spectrometer (ThermoFisher, San Jose, CA, USA). Field emission scanning electron microscope (FESEM) images were obtained using a FE-SEM S-4800 instrument (Hitachi, Ltd., Tokyo, Japan). Samples were prepared by spinning the samples on glass slices and coating with Pt. Powder X-ray diffractions were generated by using a Philips PW3830 (Philips, Ltd., Eindhoven, Holland) with a power of 40 kV at 40 mA (Cu target,  $\lambda = 0.1542$  nm). UV-vis absorption spectra were recorded on a UV-vis 2550 spectroscope (Shimadzu, Ltd., Tokyo, Japan). Fluorescence spectra were recorded on an Edinburgh Instruments FLS 900 (Edinburgh Instruments, Ltd, Livingston, UK). Fourier transform infrared (FTIR) spectra were collected using a Nexus 470 spectrometer (Nicolet Company) with a resolution of  $2\text{ cm}^{-1}$ , and 32 scans were accumulated to obtain an acceptable S/N ratio. The samples were prepared with KBr pellets. Original spectra were baseline-corrected using Omnic 5.1 software. The optimized structures and fluorescence emission of molecule **1** and the dimer **1** were determined with the help of theoretical calculations, in the framework of density functional theory (DFT) calculations at the level of B3LYP-D3/6-31G\* in a suite of Gaussian 09 programs.<sup>34</sup>

## Results and discussion

The synthesis and characterization of quinoline derivative **1** is described in the Supporting Information. The gelation behavior of compound **1** was evaluated in various organic solvents by a normal heating-cooling process. It was found that the stable organogels were formed in ethanol, acetonitrile, n-hexane, petroleum ether and DMSO with the critical gel concentration (CGC) of 3.17%, 0.45%, 0.16%, 0.17% and 0.57%, respectively. The organogel in petroleum ether was transparency, and the other four organogels were opaque (Figure S1). It was worth mentioning that the CGC of organogels **1** in n-hexane and petroleum ether was lower than 0.2 wt.%, and fell into the category of super-gelators<sup>35-37</sup>. The solutions **1** were obtained in methanol, DMF, toluene, THF,  $\text{CH}_2\text{Cl}_2$  and  $\text{CHCl}_3$  after the hot solutions were cooled to room temperature. The compound **1** was existed as the form of precipitate in 1,4-dioxane, acetone and ethyl acetate. The organogels **1** formed in the five solvents could be stable for several months. When the organogels were under 365 nm light, they could emit different intensity light. The organogels **1** formed in ethanol, hexane, petroleum ether and DMSO only emitted weak light. On the contrary, the organogel **1** in acetonitrile could emit strong light. For fluorescence chemosensor, the excellent fluorescence behavior provided a good platform for application in sensor field through fluorescence change.

**Table 1** The gelation ability of molecule **1** in different solvents.<sup>a</sup>

Solvent	3-57
methanol	S
ethanol	G (3.17%)
DMF	S
acetonitrile	G (0.45%)
1,4-dioxane	P
n-hexane	G (0.16%)
acetone	P
toluene	S
ethyl acetate	P
petroleum ether	G (0.17%)
DMSO	G (0.57%)
THF	S
CH <sub>2</sub> Cl <sub>2</sub>	S
CHCl <sub>3</sub>	S

S = solution; P = precipitate; G = gel; the values in the brackets denote the CGC.

Low weight organic molecule could be self-assembled into the different morphologies under the driving force of the noncovalent interaction. The self-assembly structures of **1** in five kinds of solvents were investigated one by one through field emission scanning electron microscopy (FESEM). Nanofibers structure was observed in organogel **1** in ethanol with the length of tens of microns and width of about 300 nm (Figure 1a). The similar fibers structure was found in organogel **1** in acetonitrile with the length of tens of microns and width of about 400 nm (Figure 1b). The wrinkled structure with many irregular pores inlaying it was formed in organogel **1** in n-hexane (Figure 1c). A relatively smooth film structure was formed in the self-assembly process of compound **1** in petroleum ether (Figure 1d). The similar fishing net structure knitted by nanofibers was observed in organogel **1** in DMSO (Figure 1e). From the above results, it showed that compound **1** could self-assemble into different structure in different solvents.

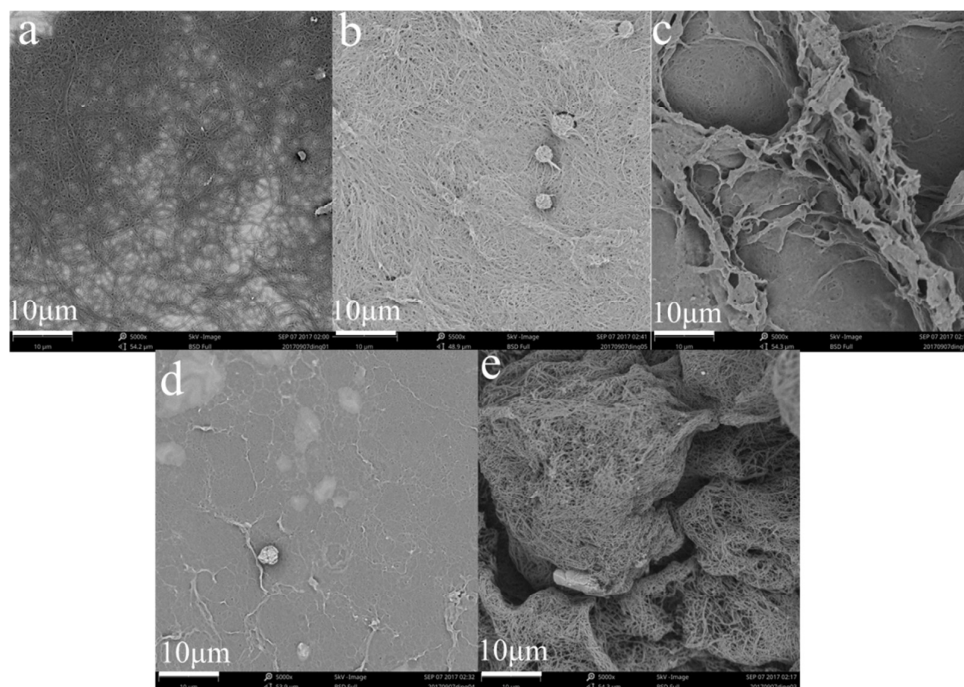


**Figure 1** SEM images of organogels **1** in different solvents of ethanol (a), acetonitrile (b), n-hexane (c), petroleum ether (d) and DMSO (e). The scale bars for images a, b, c, d and e are all 10  $\mu\text{m}$ . The organogel concentration was all at their CGC.

UV-vis absorption spectra of solution and gel state could provide the information about the self-assembly process. The UV-vis absorption spectra of compound **1** in solution and gel state were carried out and showed in Figure 2. The UV-vis absorption spectrum of solution **1** in ethanol showed two absorption bands at 270 and 332 nm which should be assigned to the  $n-\pi^*$  electron transition of quinoline group (Figure 2a)<sup>38</sup>. Comparing with **1** ethanol solution, the two absorption bands of gel **1** in ethanol at 271 and 332 nm did not have any obvious shift expect for two new absorption bands at 348 and 379 nm appearing. The absorption bands of gel **1** in acetonitrile were at 263, 343 and 382 nm (Figure 2b). The absorption band at 263 nm had a blue-shift of 7 nm, and the absorption band at 343 had a red-shift of 11 nm comparing with that of **1** acetonitrile solution which showed that  $\pi-\pi$  stacking interaction existed in gel state. For solution and gel **1** in hexane, the UV-vis absorption spectra exhibited the similar absorption behavior, and there was no shift between solution and gel state (Figure 2c). The UV-vis absorption spectrum of **1** in petroleum ether solution had three absorption bands at 270, 332 and 350 nm. The UV-vis absorption bands of organogel **1** in petroleum were broadened without any shift (Figure 2d).

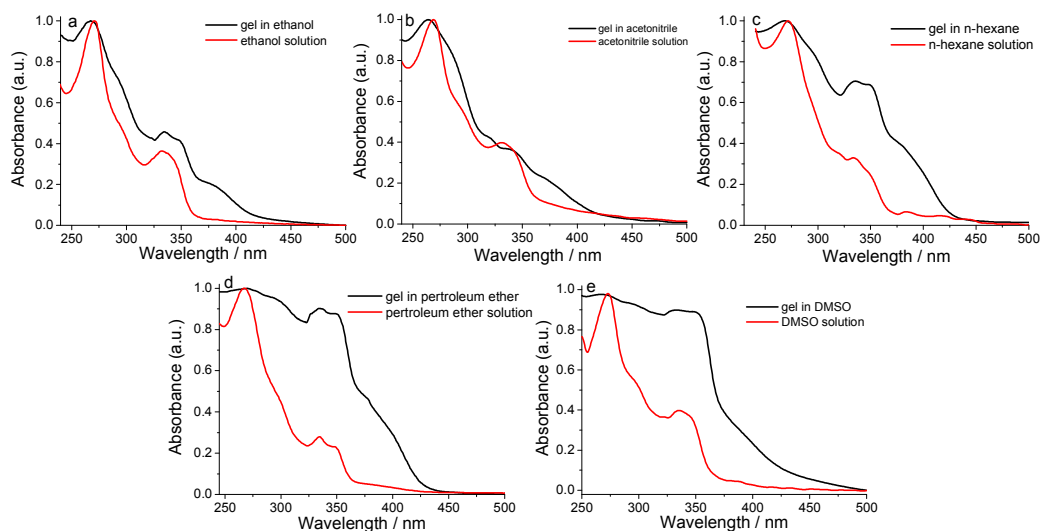


**Figure 2** UV-vis absorption spectra of **1** in solution and gel state from different solvents of ethanol (a), acetonitrile (b), n-hexane (c), petroleum ether (d) and DMSO (e). The solution concentration of **1** was all  $10^{-5}$  M. The organogel concentration was all at their corresponding CGC.

For organic functional materials, fluorescence emission behaviors were very important properties. The fluorescence emission spectra of compound **1** in solution and gel state from different solvents were studied and showed in Figure 3. The compound **1** in ethanol solution and gel state formed in ethanol all emitted 382 nm light under the excitation of 332 nm light which showed no obvious  $\pi$ - $\pi$  stacking in gel state (Figure 3a). For compound **1** in acetonitrile solution, it could also emit 382 nm light under the same condition (Figure 3b). When compound **1** was self-assembled into organogel **1** in acetonitrile, organogel **1** in acetonitrile exhibited different fluorescence emission behavior with the two emission peaks at 385 nm and 495 nm which showed the  $\pi$ - $\pi$  stacking interaction existed in gel state. In order to understand the fluorescence behavior change in its gel state, the fluorescence emission of single molecule and dimer of **1** was investigated via theoretical calculation (Figure S2). The theoretical calculation results showed the fluorescence emission peak of the single molecule **1** was located at 367 nm, and that of the dimer of **1** was at 467 nm which clearly verified the fluorescence emission behavior of molecule **1** in solution and gel state. The molecule distance in the dimer of **1** was about 3.37 Å. When compound **1** in hexane was self-assembled into organogel **1**, the maximum fluorescence emission peak was red-shifted from 380 nm of **1** hexane solution to 386 nm<sup>33</sup>. For organogels **1** from petroleum ether and DMSO, the maximum fluorescence emission peak was all at 385 nm, and the fluorescence emission peak of their corresponding solution was still basically at 385 nm without any obvious shift.

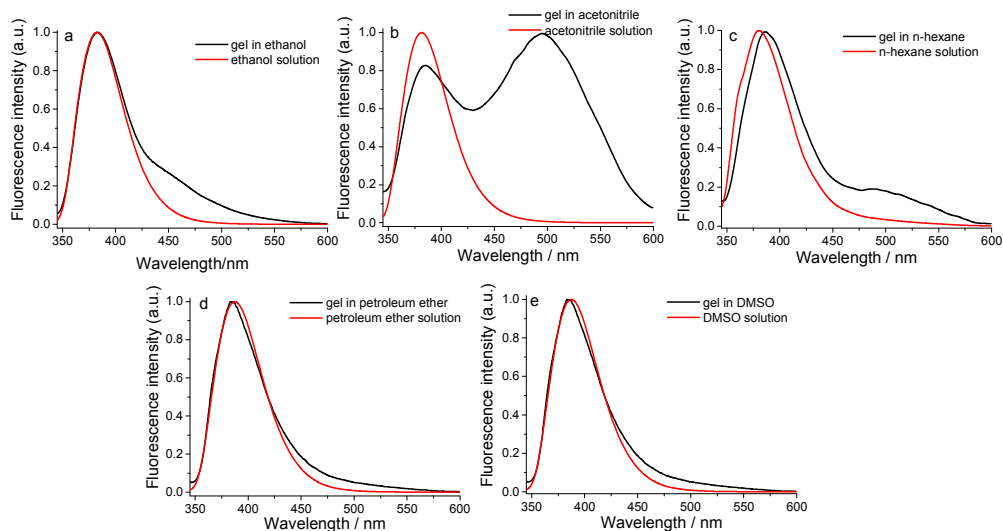


**Figure 3** Fluorescence emission spectra ( $\lambda_{\text{ex}} = 332 \text{ nm}$ ) of **1** in solution and gel from different solvents of ethanol (a), acetonitrile (b), n-hexane (c), petroleum ether (d) and DMSO (e). The solution concentration of **1** was all  $10^{-5} \text{ M}$ . The organogel concentration was all at their corresponding CGC.

FT-IR spectrum could provide some important information of the self-assembly system, especially for hydrogen bonding interaction. The FT-IR spectra of xerogels **1** formed different solvents were investigated one by one (Figure 4). As showed in Figure 4, the broadbands of N-H stretching vibration of xerogels **1** formed in hexane, acetonitrile, ethanol, petroleum ether and DMSO were at 3293, 3293, 3289, 3293 and 3285  $\text{cm}^{-1}$ , respectively which indicated of possible hydrogen bonding<sup>39</sup>. For C=O stretching vibration in xerogel from hexane, acetonitrile, ethanol, petroleum ether and DMSO, the C=O stretching vibration bands of xerogels **1** formed in different solvents were at 1639, 1639, 1634, 1639 and 1639  $\text{cm}^{-1}$ , respectively which further proved the hydrogen bonding interaction existed in self-assembly system<sup>40</sup>.

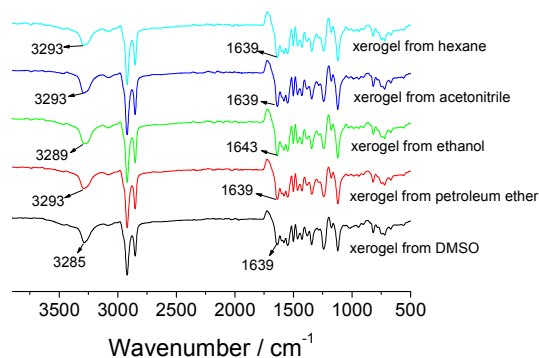


**Figure 4** FTIR spectra of xerogels **1** from different solvents. The organogel concentration was all at their corresponding CGC.

To provide further information about the self-assembly behavior, dried xerogels **1** formed from the five solvents were subjected to powder X-ray diffraction (Figure 5). The scattering pattern of xerogel **1** in ethanol

shows broad peaks in the wide angle range corresponding to d-spacing of about 0.98 nm and 0.42 nm, closely to equivalent patterns for xerogels **1** derived from acetonitrile, hexane and petroleum ether (Figure 5a). The XRD patterns of xerogel **1** in acetonitrile, hexane and petroleum ether exhibited the diffraction peaks with the corresponding spacing of about 0.98nm, 0.41nm, 1.01nm, 0.42nm, 1.02nm and 0.42 nm, respectively (Figure 5b-5d). It was different that XRD pattern of xerogel **1** formed in DMSO showed a series of peaks with the d-spacing of 2.13 nm, 1.07 nm, 0.64 nm and 0.43 nm (Figure 5e). To a large extent, the ratio of the d-spacing of 2.13 nm, 1.07 nm and 0.43 nm follows the proportion 1: 1/2: 1/4, suggesting that the gelators were combined into a bilayer arrangement<sup>41</sup>. According to the above experiments results, the probably packing mode of gelator was speculated and listed in Figure 6. The molecule **1** was firstly stacking into a fibre structure, the fibres were further intertwined and formed three-dimensional network.

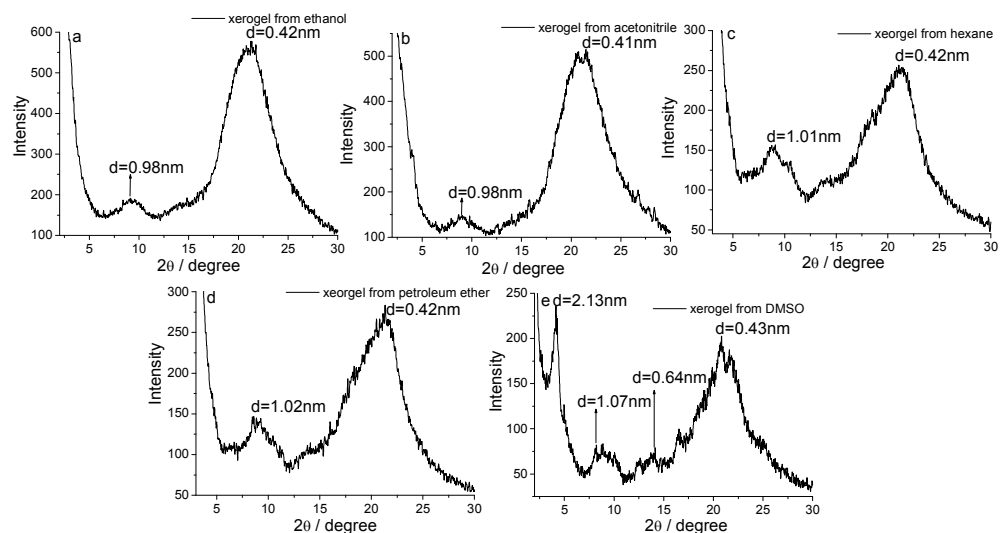


**Figure 5** XRD patterns of xerogels **1** in solution and gel from different solvents of ethanol (a), acetonitrile (b), n-hexane (c), petroleum ether (d) and DMSO (e). The solution concentration of **1** was all  $10^{-5}$  M. The organogel concentration was all at their corresponding CGC.

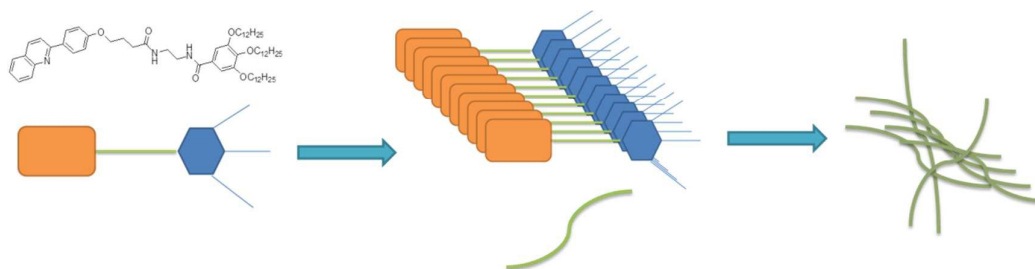


**Figure 6** The probably self-assembly mode of molecule **1**.

It was well known that materials surface wettability was decided by the composition of the material itself and materials surface roughness which was one important property which also reflected the self-assembly behavior of

the surface layer<sup>42-45</sup>. For supramolecular self-assembly system, a various of structures could be obtained in the self-assembly process such as nanofibre, tube, ribbon, piece, sphere, vesica and film. The different wettability could be observed in supramolecular self-assembly system, even if in a single component self-assembly system. For example, the nanofiber structure was observed in organogel **1** derived from five solvents (Figure 1), but the structure surface wettability was completely different as showed in Figure 7. The xerogel **1** film surface formed in ethanol had some hydrophobicity with water contact angle of 98.5°. On the contrary, the xerogel **1** film surface formed in acetonitrile exhibited high hydrophobicity with the water contact angle of 147°. When xerogel **1** film surfaces formed in n-hexane and petroleum ether were subjected to water contact angle experiment, they also exhibited some weak hydrophobicity with the water contact angle of 94° and 92°. Xerogel **1** film surfaces formed in DMSO also exhibited high hydrophobicity with the contact angle of 146.5° (Figure 7e). From the above results, self-assembly of compound **1** was utilized a different mode in different solvent.

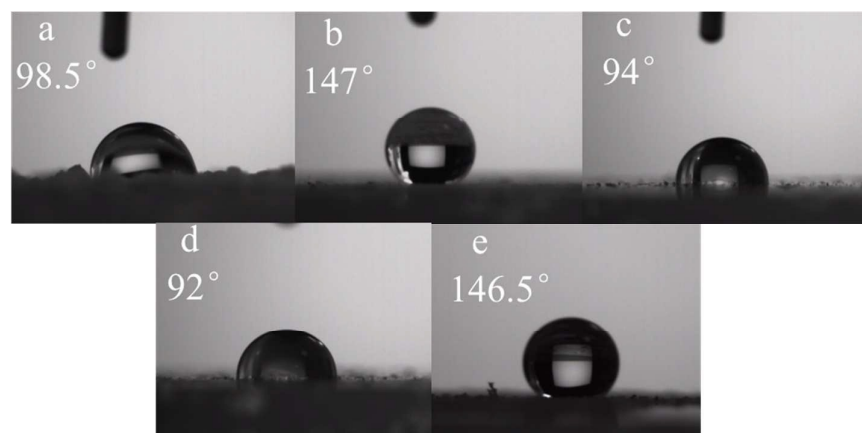


**Figure 7** Water contact angle experiments results of the film coating with gel **1** from different solvents of ethanol (a), acetonitrile (b), n-hexane (c), petroleum ether (d) and DMSO (e). The organogel concentration was all at their corresponding CGC.

The fluorescence emission change of compound **1** in acetonitrile solution was investigated under response to volatile acid and organic amine. Firstly, the selectivity of compound **1** towards volatile acid and organic amine was investigated in solution state. As showed in the Figure 3S a, the fluorescence emission intensity of solution **1** was decreased with the addition formic acid, hydrochloric acid, acetic acid, propionic acid and trifluoroacetic acid (TFA). In the five kinds of acid, it was different that the fluorescence emission peak at 381 nm was completely disappeared, and a new emission peak at 460 nm was appeared under addition of TFA which exhibited compound **1** had a good selectivity toward TFA. For solution **1** with addition of TFA, the emission peak at 381 nm could be come back under addition of diethylamine, ethylenediamine, TEA and ammonia which showed solution **1** with addition TFA could respond to aliphatic amine (Figure 3Sb). When the same amount of aniline was added to

solution **1** with addition of TFA, the fluorescence emission change did not like the other organic amine and not return to its original emission properties of solution **1** which showed that solution **1** with addition of TFA fully responded toward aniline.

The trifluoroacetic acid (TFA) and triethylamine (TEA) was selected as volatile acid and organic amine, respectively. As showed in Figure 8a, the fluorescence emission intensity at 382 nm was gradually decreased, a new emission peak at 458 nm was appeared and the emission intensity was gradually increased accompanying with a well defined isosbestic point at 431 nm. When 0.11 eq. of TFA was added to **1** acetonitrile solution, the fluorescence emission did not change and reached the terminal point (Figure 8a). Plotting the fluorescence intensity change of **1** at 381 nm as a function of  $1/[TFA]$  ( $1/[I-I_0]$  vs  $1/[TFA]$ ) gave a linear curve. The binding constant was determined to be  $7.53 \times 10^6 \text{ M}^{-1}$  (the details showed in the SI, figure S4). The detection limit was  $5.68 \times 10^{-9} \text{ M}$  (Table S1 and Figure S5 in the SI). In order to prove the reversibility of fluorescence emission of compound **1**, the fluorescence emission of **1** solution with addition of 0.11 eq. of TFA was further investigated under further addition of TEA (Figure 8b). With addition of TEA, the fluorescence emission intensity at 382 nm was gradually recovered and the fluorescence emission intensity at 458 nm was gradually decreased. As showed in Figure 8c, the fluorescence emission could be reversibly transformed between 382 nm and 458 nm at least for 6 times. It was well known that fluorescence sensor is especially attractive for recognition of analytes because its fast, real-time responses and high sensitivity and without expensive equipment<sup>23</sup>. The supramolecular self-assembly gel materials with aggregation-induced emission (AIE) properties could have great potential application via the formation of luminescent aggregation, to make up for the shortcoming of no emission in solution state. Herein, xerogel **1** film formed in acetonitrile was used to respond to volatile acid and organic amine vapors (Figure 8d). The fluorescence emission of xerogel **1** had the similar emission behavior like that of organogel **1** in acetonitrile except for the relative decreasing at the fluorescence emission intensity of peak at 382 nm. When xerogel **1** respond to TFA, the fluorescence emission peak at 494 nm was disappeared in one minute. At the same time, the fluorescence emission properties of xerogel **1** also could be recovered in one minute after removing of TFA. The fluorescence emission change process of xerogel **1** under response to TFA was made into a movie **1** as the supporting information. When xerogel **1** with response to TFA was further responded to TEA, the fluorescence emission peak of xerogel **1** was shifted from 383 nm to 436 nm in one minute which showed that fluorescence emission of xerogel **1** was disturbed by triethylamine trifluoroacetate formed in the response process. The fluorescence emission change process of xerogel **1** under response to TFA and TEA was made into a movie **2** as the supporting information. From the above experiment results, the xerogel **1** film could fast respond to TFA and

TEA. In this work, xerogel **1** could emit different light under response to TFA and TEA, not like the turn-on fluorescence xerogel film sensor.

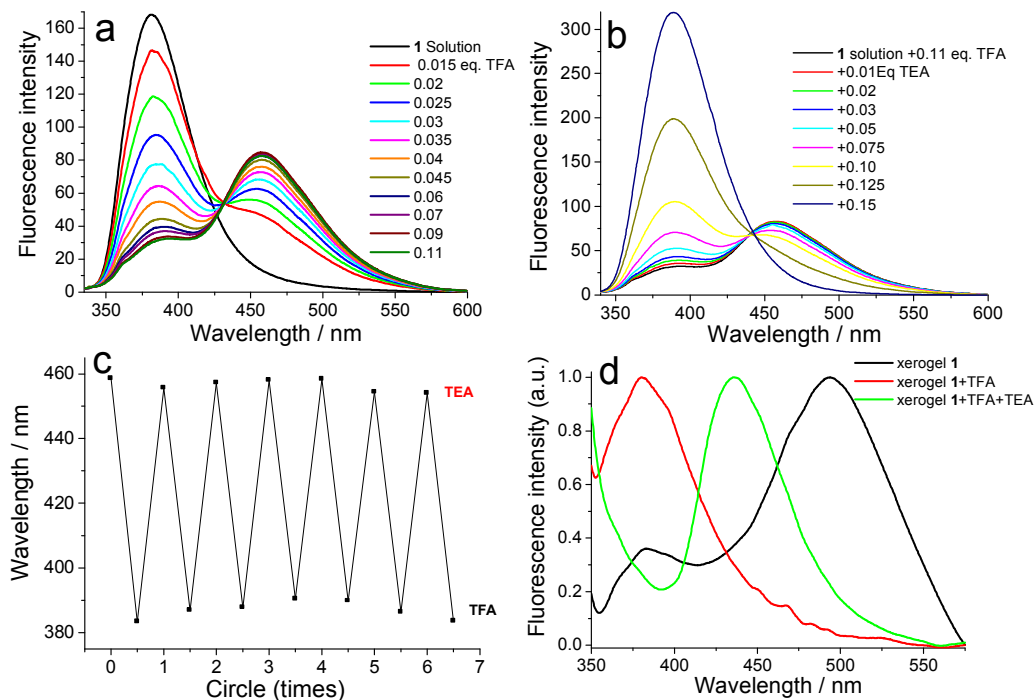


**Figure 8** (a) Fluorescence emission change of **1** acetonitrile solution under titration of TFA; (b) Fluorescence emission change of **1** acetonitrile solution with addition of 0.11 eq. of TFA under titration of TEA; (c) Fluorescence emission reversibility cycle number of **1** acetonitrile solution under addition of TFA and TEA; (d) Fluorescence emission change of xerogel **1** from acetonitrile after response to TFA and TEA.

## Conclusion

The present results showed that the organogels **1** could be formed in five kinds of solvents by the new gelator based on derivative. The organogels **1** from five kinds of solvents were characterized by FESEM, UV-vis, FL, XRD, FTIR and water contact angle experiment. The results indicated that different self-assembly behavior were observed in different solvents, and formed different structure with different wettability from super-hydrophilicity to super-hydrophobic under. Hydrogen-bonding interaction could be found by FTIR spectra of xerogels **1**. The organogel **1** driven from acetonitrile could emit much stronger light than that of organogels formed in the other four solvents. Interestingly, compound **1** acetonitrile solution could reversibly respond to TFA and TEA, and accompanied by the reversible change of fluorescence emission. At the same time, xerogel **1** formed in acetonitrile could sensitively and reversibly respond to TFA and TEA vapour. The fluorescence emission of xerogel **1** was changed from cyan into blue after response to TFA in one minute. When TEA was further added, the fluorescence

emission could be fast backed from blue to its original cyan light in one minute. This soft material with remarkable responsive ability of volatile acid and organic amine vapor provides its potential application in a variety of advanced smart materials.

### Acknowledgment

The authors thanks for the financial support by the National Natural Science Foundation of China (U1704164, 21401159 and 21501031), Institute for Conservation and Utilization of Agro-bioresources in Dabie Mountains, Funding scheme for the young backbone teachers of higher education institutions in Henan Province (2015GGJS-141), the Science & Technology Innovation Talents in Universities of Henan Province (No. 17HASTIT005) and the Nanhu Scholars Program for Young Scholars of XYNU.

### Reference

1. S. A. P. van Rossum, M. Tena-Solsona, J. H. van Esch, R. Eelkema and J. Boekhoven, Dissipative out-of-equilibrium assembly of man-made supramolecular materials. *Chem. Soc. Rev.*, 2017, **46**, 5519-5535.
2. M. X. Kuang, J. X. Wang and L. Jiang, Bio-inspired photonic crystals with superwettability. *Chem. Soc. Rev.*, 2016, **45**, 6833-6854.
3. B. O. Okesola and D. K. Smith, Applying low-molecular weight supramolecular gelators in an environmental setting – self-assembled gels as smart materials for pollutant removal. *Chem. Soc. Rev.*, 2016, **45**, 4226-4251.
4. C. Zhong, Y. D. Deng, W. B. Hu, J. L. Qiao, L. Zhang and J. J. Zhang, A review of electrolyte materials and compositions for electrochemical supercapacitors. *Chem. Soc. Rev.*, 2015, **44**, 7484-7539.
5. L. M. de Espinosa, W. Meesorn, D. Moatsou and C. Weder, Bioinspired polymer systems with stimuli-responsive mechanical properties. *Chem. Rev.*, 2017, **117**, 12851-12892.
6. E. Yashima, N. Ousaka, D. Taura, K. Shimomura, T. Ikai and K. Maeda, Supramolecular helical systems: helical assemblies of small molecules, foldamers, and polymers with chiral amplification and their functions. *Chem. Rev.*, 2016, **116**, 13752–13990
7. M. H. Liu, L. Zhang and T. Y. Wang, Supramolecular chirality in self-assembled systems. *Chem. Rev.*, 2015, **115**, 7304-7397.
8. S. Bhattacharya and S. K. Samanta, Soft-nanocomposites of nanoparticles and nanocarbons with supramolecular and polymer gels and their applications. *Chem. Rev.*, 2016, **116**, 11967-12028
9. S. S. Babu, V. K. Praveen and A. Ajayaghosh, Functional  $\pi$ -gelators and their applications. *Chem. Rev.*, 2014,

- 114, 1973-2129.
10. B.-K. An, J. Gierschner and S. Y. Park,  $\pi$ -Conjugated cyanostilbene derivatives: a unique self-assembly motif for molecular nanostructures with enhanced emission and transport. *Acc. Chem. Res.*, 2012, **45**, 544-554.
  11. M. George and R. G. Weiss, Molecular organogels. soft matter comprised of low-molecular-mass organic gelators and organic liquids. *Acc. Chem. Res.*, 2006, **39**, 489-497.
  12. Z. Wei, J. H. Yang, J. X. Zhou, F. Xu, M. Zrinyi, P. H. Dussault, Y. Osada and Y. M. Chen, Self-healing gels based on constitutional dynamic chemistry and their potential applications. *Chem. Soc. Rev.*, 2014, **43**, 8114-8131.
  13. M. D. Segarra-Maset, V. J. Nebot, J. F. Miravet and B. Escuder, Control of molecular gelation by chemical stimuli. *Chem. Soc. Rev.*, 2013, **42**, 7086-7098.
  14. C. Tomasini and N. Castellucci, Peptides and peptidomimetics that behave as low molecular weight gelators. *Chem. Soc. Rev.*, 2013, **42**, 156-172.
  15. V. S. Balachandran, S. R. Jadhav, P. K. Vemula and G. John, Recent advances in cardanol chemistry in a nutshell: from a nut to nanomaterials. *Chem. Soc. Rev.*, 2013, **42**, 427-438.
  16. H. J. Jiang, L. Zhang, J. Chen and M. H. Liu. Hierarchical self-assembly of a porphyrin into chiral macroscopic flowers with superhydrophobic and enantioselective property. *ACS Nano*, 2017, **11**, 12453-12460.
  17. Q. X. Jin, L. Zhang and M. H. Liu. Solvent-polarity-tuned morphology and inversion of supramolecular chirality in a self-assembled pyridylpyrazole-linked glutamide derivative: nanofibers, nanotwists, nanotubes, and microtubes. *Chem. Eur. J.*, 2013, **19**, 9234-9241.
  18. X. H. Yan, P. L. Zhu and J. B. Li, Self-assembly and application of diphenylalanine-based nanostructures. *Chem. Soc. Rev.*, 2010, **39**, 1877-1890.
  19. X. H. Cao, N. Zhao, H. T. Lv, Q. Q. Ding, A. P. Gao, Q. S. Jing and T. Yi, Strong blue emissive supramolecular self-assembly system based on naphthalimide derivatives and its ability of detection and removal of 2,4,6-trinitrophenol. *Langmuir*, 2017, **33**, 7788-7798.
  20. X. H. Cao, Q. Q. Ding, N. Zhao, A. P. Gao, Q. S. Jing, Supramolecular self-assembly system based on naphthalimide boric acid ester derivative for detection of organic amine. *Sensors and Actuators B*, 2018, **256**, 711-720.
  21. X. H. Cao, T. T. Zhang, A. P. Gao, K. L. Li, Q. L. Cheng, L. J. Song and M. Zhang, Aliphatic amine responsive organogel system based on a simple naphthalimide derivative. *Org. Biomol. Chem.*, 2014, **12**,

- 6399-6405.
22. H. W. Lin, M. Jang and K. S. Suslick, Dual supramolecular photochirogenesis: ultimate stereocontrol of photocyclodimerization by a chiral scaffold and confining host. *J. Am. Chem. Soc.*, 2011, **133**, 16786-16789.
  23. Z. L. Tang, J. H. Yang, J. Y. Yu and B. Cui, A colorimetric sensor for qualitative discrimination and quantitative detection of volatile amines. *Sensors*, 2010, **10**, 6463-6476.
  24. Y. Chen, K. Ma, T. Hu, B. Jiang, B. Xu, W. J. Tian, J. Z. Sun and W. K. Zhang, Investigation of the binding modes between AIE-active molecules and dsDNA by single molecule force spectroscopy, *Nanoscale*, 2015, **7**, 8939-8945.
  25. X. L. Pang, X. D. Yu, H. C. Lan, X. T. Ge, Y. J. Li, X. L. Zhen and T. Yi, Visual recognition of aliphatic and aromatic amines using a fluorescent gel: application of a sonication-triggered organogel. *ACS Appl. Mater. Interfaces*, 2015, **7**, 13569-13577.
  26. P. C. Xue, J. P. Ding, Y. B. Shen, H. Q. Gao, J. Y. Zhao, J. B. Sun and R. Lu, Aggregation-induced emission nanofiber as a dual sensor for aromatic amine and acid vapor. *J. Mater. Chem. C*, 2017, **5**, 11532-11541.
  27. X. H. Cao, N. Zhao, G. D. Zou, A. P. Gao, Q. Q. Ding, G. J. Zeng and Y. Q. Wu, A dual response organogel system based on an iridium complex and a Eu(III) hybrid for volatile acid and organic amine vapors. *Soft Matter*, 2017, **13**, 3802-3811.
  28. J. Yin, Y. Hua and J. Y. Yoon, Fluorescent probes and bioimaging: alkali metals, alkaline earth metals and pH. *Chem. Soc. Rev.*, 2015, **44**, 4619-4644.
  29. H. Xu, R. F. Chen, Q. Sun, W. Y. Lai, Q. Q. Su, W. Huang and X. G. Liu, Recent progress in metal-organic complexes for optoelectronic applications. *Chem. Soc. Rev.*, 2014, **43**, 3259-3302.
  30. D.J. Fanna, Y. J. Zhang, L. Li, I. Karatchevtseva, N. D. Shepherd, A. Azim, J. R. Price, J. Aldrich-Wright, J. K. Reynolds and F. Li, 3d transition metal complexes with a julolidine-quinoline based ligand: structures, spectroscopy and optical properties. *Inorg. Chem. Front.*, 2016, **3**, 286-295.
  31. Y. C. Cai, C. Li and Q. H. Song, Selective and visual detection of a nerve agent mimic by phosphorylation and protonation of quinolin oximes. *J. Mater. Chem. C*, 2017, **5**, 7337-7343.
  32. Y. W. Dong, R. Q. Fan, W. Chen, P. Wang and Y. L. Yang, A simple quinolone Schiff-base containing CHEF based fluorescence 'turn-on' chemosensor for distinguishing Zn<sup>2+</sup> and Hg<sup>2+</sup> with high sensitivity, selectivity and reversibility. *Dalton Trans.*, 2017, **46**, 6769-6775.
  33. X. H. Cao, L. Y. Meng, Z. H. Li, Y. Y. Mao, H. C. Lan, L. M. Chen, Y. Fan and T. Yi, Large red-shifted fluorescent emission via intermolecular  $\pi$ - $\pi$  stacking in 4-ethynyl-1,8-naphthalimide-based supramolecular

- assemblies. *Langmuir*, 2014, **30**, 11753-11760.
34. M. J. Frisch, G. W. Trucks, H. B. Schlegel, G. E. Scuseria, M. A. Robb, J. R. Cheeseman, G. Scalmani, V. Barone, B. Mennucci, G. A. Petersson, H. Nakatsuji, M. Caricato, X. Li, H. P. Hratchian, A. F. Izmaylov, J. Bloino, G. Zheng, J. L. Sonnenberg, M. Hada, M. Ehara, K. Toyota, R. Fukuda, J. Hasegawa, M. Ishida, T. Nakajima, Y. Honda, O. Kitao, H. Nakai, T. Vreven, J. A. Montgomery, Jr., J. E. Peralta, F. Ogliaro, M. Bearpark, J. J. Heyd, E. Brothers, K. N. Kudin, V. N. Staroverov, R. Kobayashi, J. Normand, K. Raghavachari, A. Rendell, J. C. Burant, S. S. Iyengar, J. Tomasi, M. Cossi, N. Rega, J. M. Millam, M. Klene, J. E. Knox, J. B. Cross, V. Bakken, C. Adamo, J. Jaramillo, R. Gomperts, R. E. Stratmann, O. Yazyev, A. J. Austin, R. Cammi, C. Pomelli, J. Ochterski, R. L. Martin, K. Morokuma, V. G. Zakrzewski, G. A. Voth, P. Salvador, J. J. Dannenberg, S. Dapprich, A. D. Daniels, O. Farkas, J. B. Foresman, J. V. Ortiz, J. Cioslowski and D. J. Fox, Gaussian 09 (Revision A.02), Gaussian, Inc., Wallingford, CT, 2009.
35. A. Ajayaghosh, C. Vijayakumar, R. Varghese, S. J. George, Cholesterol-aided supramolecular control over chromophore packing: twisted and coiled helices with distinct optical, chiroptical, and morphological features. *Angew Chem Int Ed*, 2006, **45**, 456-460.
36. J. Liu, P. L. He, J. L. Yan, X. H. Fang, J. X. Peng, K. Q. Liu and Y. Fang, An organometallic super-gelator with multiple-stimulus responsive properties. *Adv Mater*, 2008, **20**, 2508-2511.
37. G. T. Wang, J. B. Lin, X. K. Jiang and Z. T. Li, Cholesterol-appended aromatic imine organogelators: a case study of gelation-driven component selection. *Langmuir*, 2009, **25**, 8414-8418.
38. C. B. Huang, L. J. Chen, J. H. Huang and L. Xu, A novel pyrene-containing fluorescent organogel derived from a quinoline-based fluorescent porphyrin: synthesis, sensing properties, and its aggregation behavior. *RSC Adv.*, 2014, **4**, 19538-19549.
39. N. Malviya, M. Das, P. Mandal and S. Mukhopadhyay. A smart organic gel template as metal cation and inorganic anion sensor. *Soft Matter*, 2017, **13**, 6243-6249.
40. X. X. Ma, Y. Q. Cui, S. W. Liu and J. C. Wu. A thermo-responsive supramolecular gel and its luminescence enhancement induced by rare earth  $Y^{3+}$ . *Soft Matter*, 2017, **13**, 8027-8030.
41. J. Chen, T. Y. Wang and M. H. Liu, A hydro-metallogel of an amphiphilic L-histidine with ferric ions: shear-triggered self-healing and shrinkage. *Inorg. Chem. Front.*, 2016, **3**, 1559-1565.
42. L. Mi, J. C. Yu, F. He, L. Jiang, Y. F. Wu, L. J. Yang, X. F. Han, Y. Li, A. R. Liu, W. Wei, Y. J. Zhang, Y. Tian, S. Q. Liu, L. Jiang, Boosting gas involved reactions at nanochannel reactor with joint gas–solid–liquid interfaces and controlled wettability. *J. Am. Chem. Soc.*, 2017, **139**, 10441-10446.

43. J. P. Hill, W. S. Jin, A. Kosaka, T. Fukushima, H. Ichihara, T. Shimomura, K. Ito, T. Hashizume, N. Ishii, T. Aida, Self-assembled hexa-peri-hexabenzocoronene graphitic nanotube. *Science*, 2004, **304**, 1481-1483.
44. M. Deng, L. Zhang, Y. Q. Jiang and M. H. Liu. Role of achiral nucleobases in multicomponent chiral self-assembly: purine-triggered helix and chirality transfer. *Angew. Chem. Int. Ed.*, 2016, **55**, 15062-15066.
45. L. Zhang, X. F. Wang, T. Y. Wang and M. H. Liu, Tuning soft nanostructures in self-assembled supramolecular gels: from morphology control to morphology-dependent functions. *Small*, 2015, **11**, 1025-1038.

## Graphical abstract:

